

Supporting Information

Two-dimensional Magnetic Bimetallic Organic Framework Nanosheets for Highly Efficient Enrichment of Phosphopeptides

Shuang Yan[§], Bin Luo[§], Jia Cheng, Lingzhu Yu, Fang Lan* and Yao Wu*

National Engineering Research Center for Biomaterials, Sichuan University, Chengdu
610064, P. R. China

E-mail: lanfang@scu.edu.cn (Fang Lan); wuyao@scu.edu.cn (Yao Wu)

MALDI-TOF MS Analysis

The sample (1 μ L) and 1 μ L of matrix (DHB 25 mg·mL⁻¹, ACN/H₂O/H₃PO₄, 70:29:1, v/v/v) were blended, deposited and air-dried on a plate. All MALDI-TOF MS data were performed by autoflex maX (Bruker Scientific, USA in reflector positive mode with a Nd : YAG laser) at 383 nm. The MALDI-TOF MS analysis was obtained in positive ion mode with a mass range of 1000-3500 m/z on the repetition rate of 1000 Hz, and an acceleration voltage of 20 kV.

LC-MS/MS Analysis and Data Search

Phosphopeptides of breast cancer cells lysate were analyzed on an EASY-nLC 1200 system (Thermo Scientific, CA) coupled with Orbitrap Fusion Lumos MS (Thermo Finnigan, San Jose, CA) with nano-electrospray ion source. Lyophilized samples were dissolved in 20 μ L TFA (1%) and loaded on thermo scientific analytical column (100 μ m \times 2 cm, 5 μ m, 100 Å, C18) and eluted and separated with analytical columns (75 μ m \times 25 cm, 5 μ m, 100 Å, C18, Thermo Co.) by mobile phase A (0.1% FA in H₂O) and mobile phase B (0.1% FA in 100% ACN) for 60 min. The linear gradient elution was carried out as follows: 5-28% mobile phase B for 0-40 min; 28-90% mobile phase B for 40-42 min; 90% mobile phase B for 42-60 min. The flow rate was 300 nL·min⁻¹. The MS was operated in positive mode. The full MS scan spectra (m/z 375-1800) were performed in Orbitrap with a resolution of 120000 (m/z 200). MS2 spectra were acquired with a resolution of 50,000 (m/z 200).

Raw data were analyzed with Proteome Discoverer 2.4. The database was Unipro_Human_20210621_202249.fasta. Search parameters were as follows: Monoisotopic mass, trypsin;

Maximum missed cleavages, 2; Charge number of peptide: 2+, 3+, and 4+, Carbamidomethylation (C) was set as fixed modification; Variable modifications (M); Acethyl(protein N-term), Phospho (STY); Precursor-ion mass tolerance, 10 ppm; Fragment-ion mass tolerance, 0.05 Da.

DFT Theoretical Calculations

All of spin-polarized calculations based on density functional theory (DFT) were performed by utilizing Dmol3 package ¹. The generalized gradient approximation (GGA) in the Perdew-Burke-Ernzerhof form and Semicore Pseudopotential method (DSPP) with the double numerical basis sets plus the polarization functional (DNP) were adopted ²⁻³. The double numerical basis sets plus the polarization functional (DNP) were adopted. A DFT-D correction with Grimme scheme was used to account for the dispersion interaction ⁴. The SCF convergence for each electronic energy was set as 1.0×10^{-6} Ha, and the geometry optimization convergence criteria were set up as follows: 1.0×10^{-6} Ha for energy, $0.001 \text{ Ha} \cdot \text{\AA}^{-1}$ for force, and 0.001 \AA for displacement, respectively. Bond energy were examined by linear and quadratic synchronous transit methods in combination with the conjugated gradient (CG) refinement. Finally, the adsorption energies (E_{ads}) are calculated as $E_{\text{ads}} = E_{\text{ad/sub}} - E_{\text{ad}} - E_{\text{sub}}$, where $E_{\text{ad/sub}}$, E_{ad} and E_{sub} are the optimized adsorbate/substrate system, the adsorbate in the structure and the clean substrate respectively. Moreover, the bonding energy of all structures were calculated.

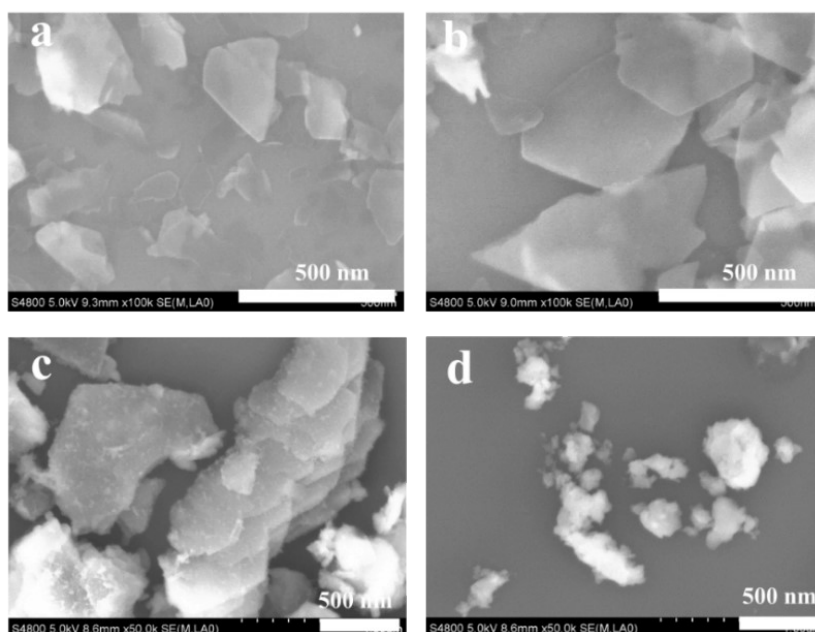


Figure S1. SEM images of the Zr-Ti BPDC nanosheets (a, $n\text{Zr}^{4+}/n\text{Ti}^{4+}=1/1$; b, $n\text{Zr}^{4+}/n\text{Ti}^{4+}=1/5$; c, $n\text{Zr}^{4+}/n\text{Ti}^{4+}=1/10$;

d, $n\text{Zr}^{4+}/n\text{Ti}^{4+}=1/20$)

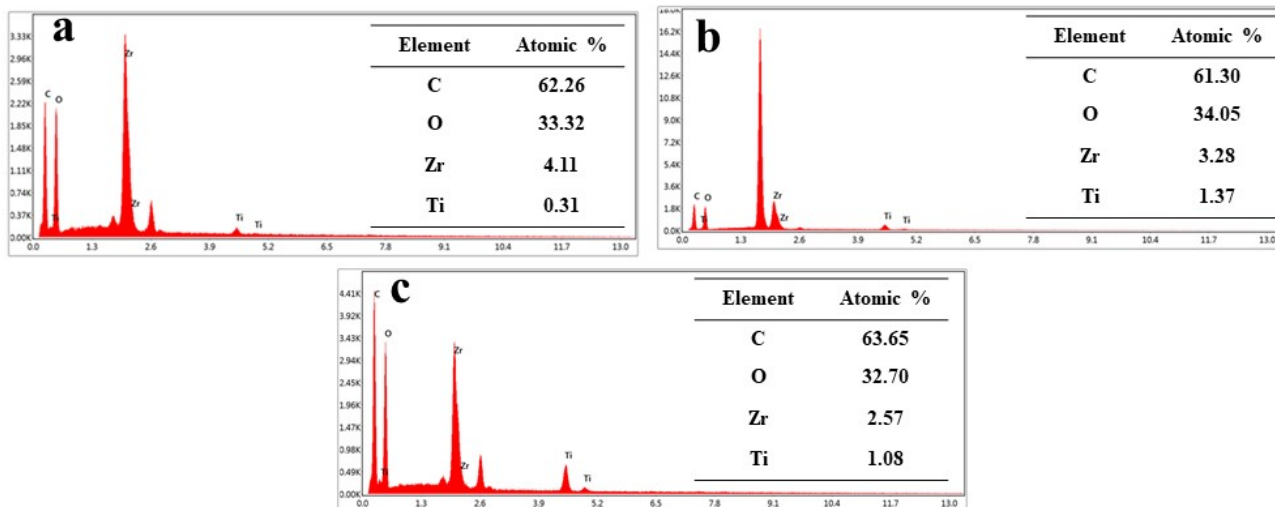


Figure S2. EDX images of the Zr-Ti BPDC nanosheets (a, $n\text{Zr}^{4+}/n\text{Ti}^{4+}=1/1$; b, $n\text{Zr}^{4+}/n\text{Ti}^{4+}=1/5$; c, $n\text{Zr}^{4+}/n\text{Ti}^{4+}=1/10$)

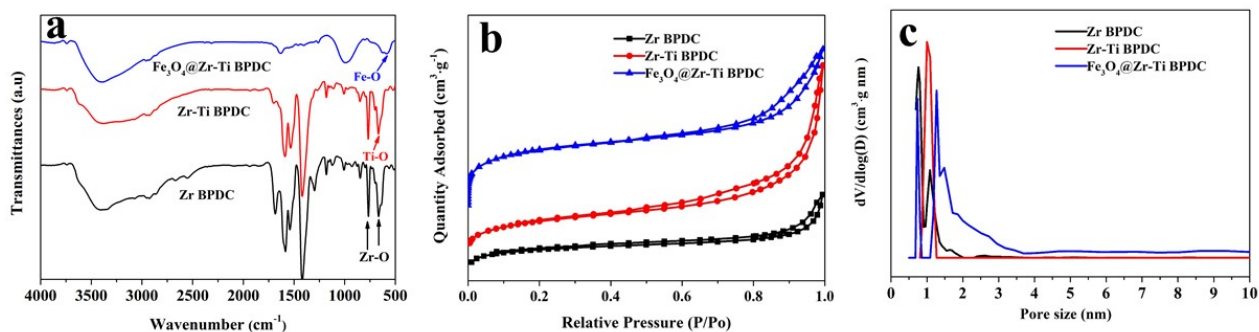


Figure S3. FTIR spectra (a) and N_2 adsorption-desorption isotherms (b) and pore size distributions (c) of Zr BPDC nanosheets, Zr-Ti BPDC nanosheets and $\text{Fe}_3\text{O}_4@$ Zr-Ti BPDC nanosheets

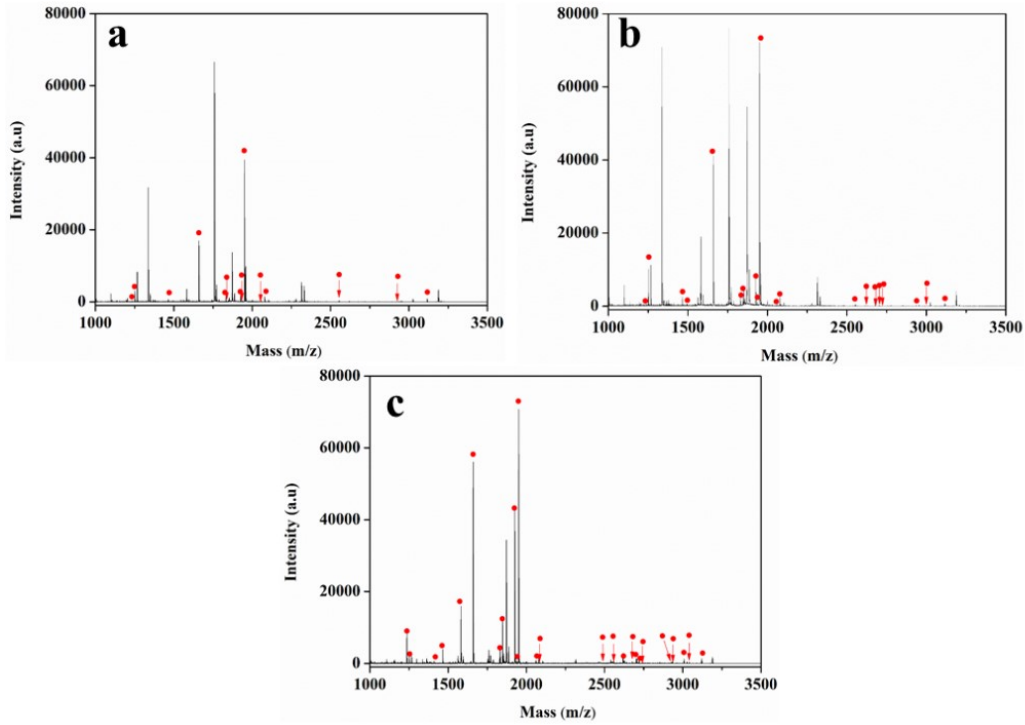


Figure S4. MALDI-TOF mass spectra of α -casein digestion (4×10^{-6} M) after enrichment by loading buffer (ACN/TFA=50%/0.1%) and elution (10% $\text{NH}_3 \cdot \text{H}_2\text{O}$), (a) $\text{Fe}_3\text{O}_4@\text{Zr-Ti}$ BPDC nanosheets ($n\text{Zr}^{4+}/n\text{Ti}^{4+}=1/1$) (b) ($n\text{Zr}^{4+}/n\text{Ti}^{4+}=1/5$), (c) ($n\text{Zr}^{4+}/n\text{Ti}^{4+}=1/10$)

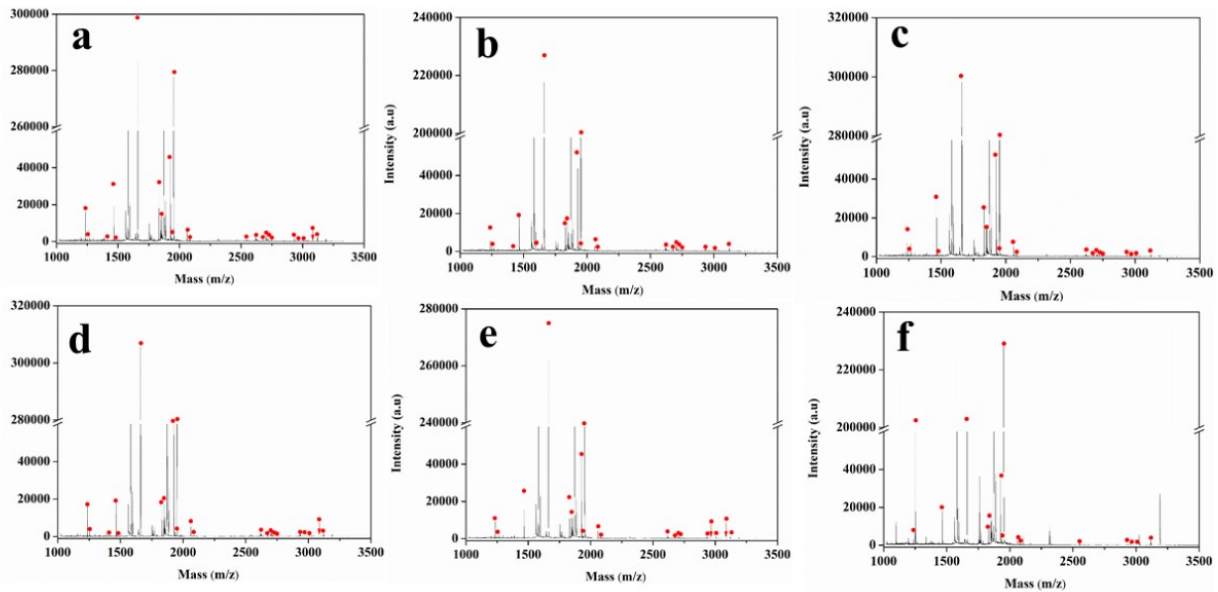


Figure S5. MALDI-TOF mass spectra of α -casein digestion (4×10^{-6} M) after enrichment by $\text{Fe}_3\text{O}_4@\text{Zr-Ti}$ BPDC nanosheets in (a, 50% ACN/0.1% TFA and 10% $\text{NH}_3 \cdot \text{H}_2\text{O}$; b, 50% ACN/0.25% TFA and 10% $\text{NH}_3 \cdot \text{H}_2\text{O}$; c, 50% ACN/0.5% TFA and 10% $\text{NH}_3 \cdot \text{H}_2\text{O}$; d, 75% ACN/0.1% TFA and 10% $\text{NH}_3 \cdot \text{H}_2\text{O}$; e, 75% ACN/0.25% TFA and 10% $\text{NH}_3 \cdot \text{H}_2\text{O}$; f, 75% ACN/0.5% TFA and 10% $\text{NH}_3 \cdot \text{H}_2\text{O}$)

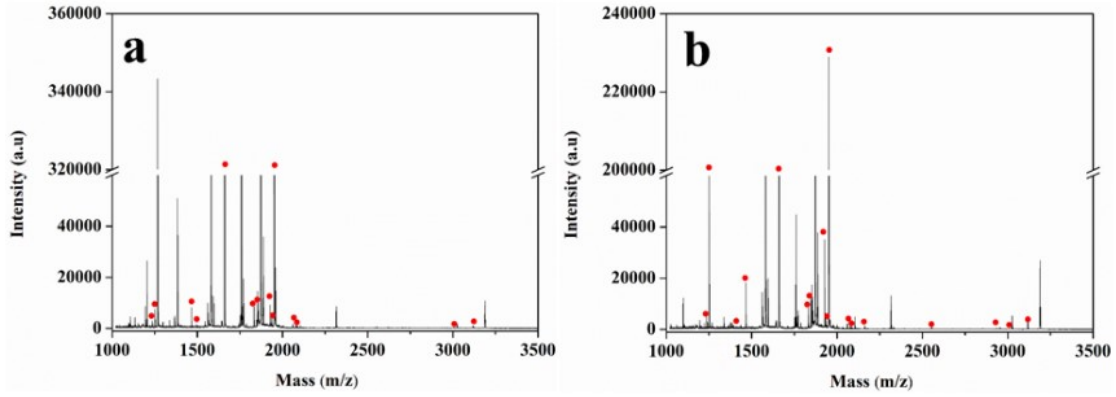


Figure S6. MALDI-TOF mass spectra of α -casein digestion (4×10^{-6} M) after enrichment by $\text{Fe}_3\text{O}_4@\text{Zr-Ti}$ BPDC nanosheets in (a, 50% ACN/0.1%TFA and 2% $\text{NH}_3 \cdot \text{H}_2\text{O}$; b, 50% ACN/0.1% TFA and 5% $\text{NH}_3 \cdot \text{H}_2\text{O}$)

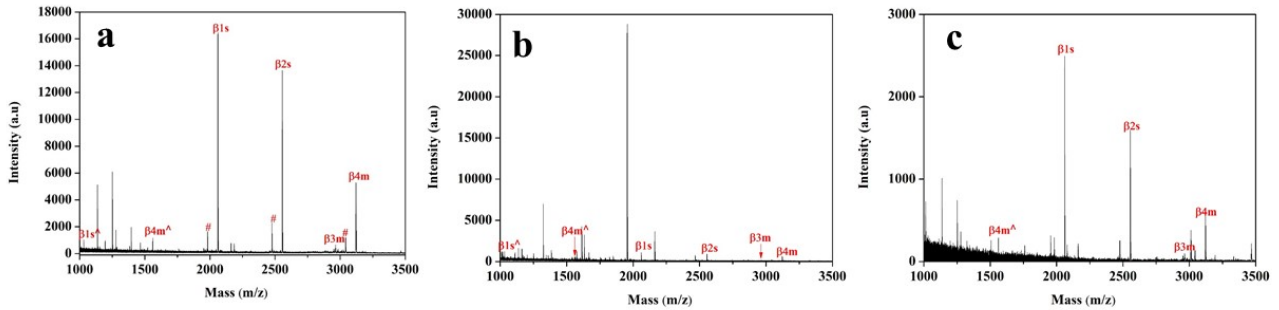


Figure S7. MALDI-TOF mass spectra of β -casein digest (4×10^{-6} M) after enrichment by $\text{Fe}_3\text{O}_4@\text{Zr-Ti}$ BPDC nanosheets. (a, cycling 1st; b, 3rd; c, 5th) (#, dephosphopeptide)

Table S1. Detail information of the observed phosphopeptides obtained from tryptic digest of α -casein after enrichment by $\text{Fe}_3\text{O}_4@\text{Zr-Ti}$ BPDC nanosheets in MALDI-TOF MS analysis

Observed m/z	Peptides sequence	Number of phosphorylation
1237.59	TVDME[pS]TEVF	1
1253.58	TVD[Mo]E[pS]TEVF	1
1412.60	EQL[pS]T[pS]EENSK	2
1467.31	TVDME[pS]TEVFIK	1
1662.02	VPQLEIVPN[pS]AEER	1
1833.33	YLGEYLIVPN[pS]AEER	1
1847.61	DIGSE[pS]TEDQAMEDIK	1
1927.90	DIG[pS]E[pS]TEDQAMEDIK	2
1943.62	DIG[pS]E[pS]TEDQA[Mo]EDIK	2
1952.09	YKVPQLEIVPN[pS]AEER	1

2062.09	FQ[pS]EEQQQTEDELQDK	1
2080.56	KYKVPQLEIVPN[pS]AEER	1
2490.02	AMKPWIQPKTKVIP[pY]VR[pY]L	2
2556.45	FQ[pS]EEQQQTEDELQDKIHPF	1
2618.90	NTMEHV[pS][pS][pS]EESII[pS]QETYSK	4
2678.36	VNEL[pS]KDIG[pS]E[pS]TEDQAMEDIK	3
2703.10	QMEAE[pS]I[pS][pS][pS]EEIVPN[pS]VEQK	5
2720.68	Q[Mo]EAE[pS]I[pS][pS][pS]EEIVPN[pS]VEQK	5
2746.90	HIQKEDVP[pS]ER[pY]LGYLEQLLR	2
2926.70	RELEELNVPGEIVESL[pS][pS][pS]EESITR	3
2934.32	KEKVNEL[pS]KDIG[pS]E[pS]TEDQAMEDIKQ	3
2966.06	RELEELNVPGEIVE[pS]L[pS][pS][pS]EESITR	4
3007.89	NANEEYSIG[pS][pS][pS]EE[pS]AEVATEEVK	4
3087.81	NANEEY[pS]IG[pS][pS][pS]EE[pS]AEVATEEVK	5
3122.02	RELEELNVPGEIVE[pS]L[pS][pS][pS]EESITR	4

Table S2. Detail information of the detected phosphopeptides obtained from tryptic digest of β -casein after enrichment by $\text{Fe}_3\text{O}_4@\text{Zr-Ti}$ BPDC nanosheets in MALDI-TOF MS analysis

Position	Observed m/z	Peptides sequence	Number of phosphorylation
$\beta 1s^{\wedge}$	1031.66	FQ[pS]EEQQQTEDELQDK	1
$\beta 4m^{\wedge}$	1561.88	RELEELNVPGEIVE[pS]L[pS] [pS][pS]EESITR	4
$\beta 1s$	2062.28	FQ[pS]EEQQQTEDELQDK	1
$\beta 2s$	2556.58	FQ[pS]EEQQQTEDELQDKIHPF	1
$\beta 3m$	2965.82	ELEELNVPGEIVE[pS]L[pS] [pS][pS]EESITR	4
$\beta 4m$	3122.93	RELEELNVPGEIVE[pS]L[pS] [pS][pS]EESITR	4

“ \wedge ” denotes doubly charged peak; “s” denotes mono-phosphopeptides; “m” denotes multi-phosphopeptides.

Table S3. List of phosphopeptides from nonfat milk digests after enrichment by $\text{Fe}_3\text{O}_4@\text{Zr-Ti}$ BPDC nanosheets in MALDI-TOF MS analysis.

m/z(Da)	Number of phosphate groups	Peptide sequence
3122.19	4	RELEELNVPGEIVE[pS]L[pS][pS][pS]EESITR
3042.30	3	RELEELNVPGEIVESL[pS][pS][pS]EESITR

3024.62	3	RELEELNVPGEIVESL[pS][pS][pS]EESITR
2966.25	4	ELEELNVPGEIVE[pS]L[pS][pS][pS]EESITR
2951.17	3	KEKVNEL[pS]KDIG[pS]E[pS]TEDQA[Mo]EDIKQ
2779.12	1	KIEKFQ[pS]EEQQQTEDELQDKIHFP
2735.06	5	Q[Mo]EAE[pS]I[pS][pS][pS]EEIVPN[pS]VEAQK
2555.88	1	FQ[pS]EEQQQTEDELQDKIHFP
2456.62	4	KNTMEHV[pS][pS][pS]EESII[pS]QET
2160.46	2	[pT]V[pY]QHOKA[Mo]KPWIQPK
2106.86		FLLQEPVLGPVRGPFPIIV
2060.75	1	FQ[pS]EEQQQTEDELQDK
1981.88	1	NMAINP[pS]KENLCSTFCK
1951.92	1	YKVPQLEIVPN[pS]AEER
1943.87	2	DIG[pS]E[pS]TEDQA[Mo]EDIK
1927.07	2	DIG[pS]E[pS]TEDQAMEDIK
1847.94	1	DIGSE[pS]TEDQAMEDIK
1832.82	1	YLGEYLIVPN[pS]AEER
1760.15		HQGLPQEVLENLLR
1660.83	1	VPQLEIVPN[pS]AEER
1561.33	4	RELEELNVPGEIVE[pS]L[pS][pS][pS]EESITR
1466.62	2	TVDME[pS]TEVFTK
1454.80	2	LSKDIG[pS]E[pS]TEDQA
1282.74	1	KKIEKFQ[pS]EEQQQTEDELQDKIHFPFAQ
1252.82	1	TVD[Mo]E[pS]TEVF
1194.92	1	NMAINP[pS]KEN
1155.60	2	[pS][pS]EEKFLR
1031.32	1	FQ[pS]EEQQQTEDELQDK

Table S4. The enrichment effect of Fe₃O₄@TiO₂, Fe-MOF and Zr-MOF

Material	LODs	Selectivity	Ref
Fe ₃ O ₄ @mTiO ₂ -80	5 fmol·μL ⁻¹	β-casein/BSA=1/500	5
Fe ₃ O ₄ @MIL-101(Fe)	8 fmol	β-casein/BSA=1/1000	6
Mag-MOF (Fe) nanofibers	0.5 fmol	β-casein/BSA=1/400	7
SPIO@SiO ₂ @MOF	0.1 fmol·μL ⁻¹	β-casein/BSA=1/400	8

SiO ₂ @PDA@Zr-MOF	4 fmol	β-casein/BSA=1/1000	9
Fe ₃ O ₄ @PDA@Zr-MOF	1 fmol	β-casein/BSA=1/500	10
Fe ₃ O ₄ @Zr-Ti BPDC nanosheets	0.4 fmol·μL ⁻¹	β-casein/Cyt C=1/1000	This work

Table S5. Comparison of Fe₃O₄@Zr-Ti BPDC nanosheets and previously reported materials for enrichment of phosphopeptides from biological sample

Materials	LODs	Real biological Samples	Number of phosphopeptides	Ref
Bi _{0.15} Fe _{0.15} TiO ₂	2×10 ⁻⁹ M	human liver lysate	116	11
MAX-Ti ₃ AlC ₂	5 fmol	BEL7402 cells lysate	830	12
mP5SOF-Arg	0.1 fmol	A594 cells lysate, mouse liver tissue lysate	450 and 1445	13
THZr-MOFs	0.05 fmol·μL ⁻¹	human serum, HeLa cell lysate	1432	14
G@mSiO ₂ -PFIL-Ti ⁴⁺	0.15 fmol	mouse brain lysate	924	15
Fe ₃ O ₄ @Zr-Ti BPDC nanosheets	0.4 fmol·μL ⁻¹	breast cancer cells lysate	2101	This work

References

1. B. Delley, *J. Chem. Phys.*, **2000**, 113, 7756-7764
2. B. Delley, *Phys. Rev. B: Condens. Matter Mater. Phys.*, **2002**, 66, 155125
3. J.P. Perdew, K. Burke, M. Ernzerhof, *Phys. Rev. Lett.*, **1996**, 77, 3865-3868
4. S. Grimme, *J. Comput. Chem.*, **2006**, 27, 1787-1799
5. Y. Zhang, W. Ma, C. Zhang, C. Wang, H. Lu, *ACS Appl. Mater. Interfaces.*, **2014**, 6, 6290-6299.
6. G. Han, Q. Zeng, Z. Jiang, W. Deng, C. Huang, Y. Li, *Talanta.*, **2017**, 171, 283-290.
7. W. W. Huan, M. Y. Xing, C. Cheng, J. Li, *ACS Sustainable Chem. Eng.*, **2019**, 7, 2245-2254
8. B. Luo, Q. Chen, J. He, Z.Y. Li, L.Z. Yu, F. Lan, Y. Wu, *ACS Sustainable Chem. Eng.* **2019**, 7, 6, 6043-6052
9. H.Z. Lin, H.M. Chen, X. Shao, C.H. Deng, *Microchim. Acta.*, **2018**, 185, 562-569
10. M. Zhao, C. H. Deng, X. M. Zhang, *Chem. Commun.*, **2014**, 50, 6228-6231
11. D.S. Zhen, C. Gao, B.D. Zhu, Q. Zhou, C.Y. Li, P. Chen, Q.Y. Cai, *Anal. Chem.*, **2018**, 90, 12414-12421

12. X.W. Li, N. Zhang, R.Z. Tang, J.W. Lv, Z. Liu, S.J. Ma, J.J. Ou, M.L. Ye, *Nanoscale.*, **2021**, 13, 2923-2930
13. H.J. Zheng, J.C. Zhang, J.T. Ma, Q. Jia, *ACS Appl. Mater. Interfaces.*, **2020**, 12, 57468-57476
14. Y.T. He, Q. Zheng, Z.A. Lin, *Microchim Acta.*, **2021**, 188, 150-160
15. B.B. Wang, W.D. Liang, H.Z. Liang, B. Liu, Q.Y. Wang, Y.H. Yan, T.T. Wang, Y.F. Jiang, Y.L. Jiang, H.D. Qiu, L.H. Lu, W. Cui, Y. Zhou, L.L. Zhao, H.B. Yu, *ACS Sustainable Chem. Eng.*, **2021**, 9, 7930-7940